agronomy

Article

Mapping of Phenological Traits in Northeast China Maize (*Zea mays* L.)

Xiaowei Wang [1], Xiaoyu Li [1], Jiatong Gu [2], Wenqi Shi [3], Haigen Zhao [1], Chen Sun [1] and Songcai You [1,*]

[1] Institute of Environment and Sustainable Development in Agriculture, Chinese Academy of Agricultural Sciences, Beijing 100081, China
[2] Agronomy College, Shenyang Agricultural University, Shenyang 110866, China
[3] College of Resources and Environment, Northeast Agriculture University, Harbin 150030, China
* Correspondence: yousongcai@caas.cn; Tel.: +86-010-82106692

Abstract: Detailed traits are required for early warning and prediction of crop-related meteorological hazards. Currently, data sets describing maize phenological traits in Northeast China are few and incomplete, resulting in poor spatial interpolation results that do not accurately reflect the spatial distributions and temporal development patterns of maize phenology in the region. In this study, a maize-phenology data set is produced containing nine phenological stages and phenological stage maps based on three sets of in situ maize-phenology data from three different sources. First, the relationship between each phenological stage and date of the previous stage, longitude, latitude, and altitude, is uncovered using a multiple stepwise regression method. Then, the spatial variation of each phenological stage using ArcGIS is explored. Finally, a maize phenological stage data set and a phenological stage atlas are established for the average state of 2010–2020 in Northeast China. The data set was validated using phenological data from agricultural weather stations run by the China Meteorological Administration. The validated data set can be used for various purposes, including real-time warning and prediction of maize-related meteorological hazards.

Keywords: *Zea mays* L.; phenology; crop management; Northeast China

check for updates

Citation: Wang, X.; Li, X.; Gu, J.; Shi, W.; Zhao, H.; Sun, C.; You, S. Mapping of Phenological Traits in Northeast China Maize (*Zea mays* L.). *Agronomy* **2022**, *12*, 2585. https://doi.org/10.3390/agronomy12102585

Academic Editors: Jitka Kumhálová, Jan Lukáš, Pavel Hamouz and Jose Antonio Dominguez-Gómez

Received: 6 September 2022
Accepted: 18 October 2022
Published: 20 October 2022

1. Introduction

Maize (*Zea mays* L.) is a cereal crop and staple food that is grown all over the world and belongs to the grasses family (Poaceae) [1]. It is commonly used in synthesizing edible oil, glucose, and many other products [2]. In recent decades, due to global warming, the sown area of maize in the northeast of China has expanded dramatically, and the planting area has gradually extended northward [3,4]. This has resulted in an increased risk of meteorological disasters occurring to maize crops and has highlighted the importance of meteorological disaster prediction for maize in the region. Take the example of drought, where crop shoot development and biomass accumulation are significantly reduced by soil water deficit at the emergence stage. Short-duration water deficit during the rapid vegetative growth period causes around 30% loss in final dry matter. The reduction in maize yield by drought can be observed in all yield components, such as kernel weight, especially for drought during or before the maize flowering stage [5]. The development of remote sensing technology and the real-time release of meteorological data has made it possible to monitor and predict maize-related meteorological hazards [6,7], but real-time monitoring needs to be supported by detailed crop information, including information on the spatial variation of the developmental stages of the crop [8]. Therefore, acquiring maize phenological information has become the key to disaster warning, prediction, and damage assessment. Current maize phenological data sets are quite incomplete in Northeast China, resulting in inaccurate spatial-interpolation results when using these data. These imperfect data sets prevent us from acquiring more accurate spatial distributions of maize phenology and phenological processes and therefore hinder routine prediction of maize weather disasters in the region.

Many scholars have conducted numerous studies on maize phenology. For example, it has been shown that the phenology of maize sown at the same time of year increases with altitude, with an increase of about 4–5 days per 100 m [9]. From 1960 to 2018, the average growing periods of early-, medium- and late-maturing common harvest maize in Northeast China were 123, 135, and 140 days, respectively [10]. Maize overall development has been extended by an average of 2.2 days per decade [11]. The seeding period of maize has been advanced in Heilongjiang Province, while it has been delayed in Liaoning and Jilin Provinces [12]. From 1981 to 2000, climate change affected crop phenology and yield, and the patterns of climate change and associated impacts were spatially diverse across China [13]. Despite these studies, most of the current research only focuses on a few specific phenological stages of maize, and their conclusions do not support the prediction of meteorological hazards for the whole range of maize phenological stages.

At present, most studies are limited by data availability, monitoring technology, and natural conditions, and it has been challenging to analyze multiple phenological stage characteristics of maize in northeastern China in terms of both time scales and spatial distributions. Following previous studies, this paper adopts a multiple stepwise regression method, combined with information on the growth and developmental patterns of maize, to obtain a fused and interpolated data set, along with associated maps, describing the nine phenological stages of maize: (1) the sowing stage (SW), (2) the emergence stage (VE), (3) the three-leaf stage (V3), (4) the seven-leaf stage (V7), (5) the jointing stage (JT), (6) the tasseling stage (VT), (7) the flowering stage (FR), (8) the silking stage (R1), and (9) the harvesting stage (R6). The fused data set is created using mathematical and statistical analyses of three sets of data collected at a total of 192 sampling locations. The new data set solves the problem of incomplete observations and limited available data records of maize phenological periods in Northeast China. It also provides the necessary data to support monitoring, early warning, and damage assessment of maize meteorological hazards in the region. In particular, our aim was to obtain an accurate data set scientifically containing the nine phenological stages of maize.

2. Materials and Methods

2.1. Study Area

The study area used in this paper includes the Heilongjiang, Jilin, and Liaoning Chinese provinces and the four leagues of the eastern part of the Inner Mongolia Autonomous Region [14]. The climatic conditions of the study area are dominated by a temperate continental monsoon climate with rainy summers and dry and cold winters. The main crops in the study area are maize, rice, and soybeans [15,16].

2.2. Data Sources

The first maize phenological data set was obtained from the China Meteorological Administration (CMA, http://data.cma.cn (accessed on 15 November 2021)) from 2010 to 2013 with 61 records of six phenological stages (i.e., SW, VE, V3, V7, JT, and R6). The VT, FR, and R1 stages were missing from this base data set.

The Institute of Environment and Sustainable Development in Agriculture, Chinese Academy of Agricultural Sciences (IEDA, CAAS) provided the second base data set consisting of a total of 99 historical records of maize phenological stages in northeastern China from 2010 to 2020. This data set had five phenological stages missing (i.e., VE, V3, V7, FR, and R1).

The third data set consisted of an additional 32 records obtained from the China National Knowledge Infrastructure (CNKI, https://www.cnki.net/ (accessed on 10 November 2021)) describing nine phenological stages (i.e., SW, VE, V3, V7, JT, VT, FR, R1, and R6), which were extracted from relevant literature for the period from 2010 to 2020.

Hence, in total a final fused data set consisting of 192 records (Table 1) was collated from the three base data sets. The spatial distribution of record locations for each base data set is shown in Figure 1.

Table 1. Details of the nine phenological stages recorded in the three base data sets used in this study (see text for details of sources). Numbers refer to the number of records per phenological stage. The location of records is shown in Figure 1. See text for explanation of each phenological stage.

Data Source	Phenological Stage								
	SW	VE	V3	V7	JT	VT	FR	R1	R6
CMA	61	60	61	60	61				61
IEDA, CAAS	99				99	99			99
CNKI	32	32	8	11	23	11	4	10	18

Note: SW: sowing stage; VE: emergence stage; V3: three-leaf stage; V7: seven-leaf stage; JT: jointing stage; VT: tasseling stage; FR: flowering stage; R1: silking stage; R6: harvesting stage.

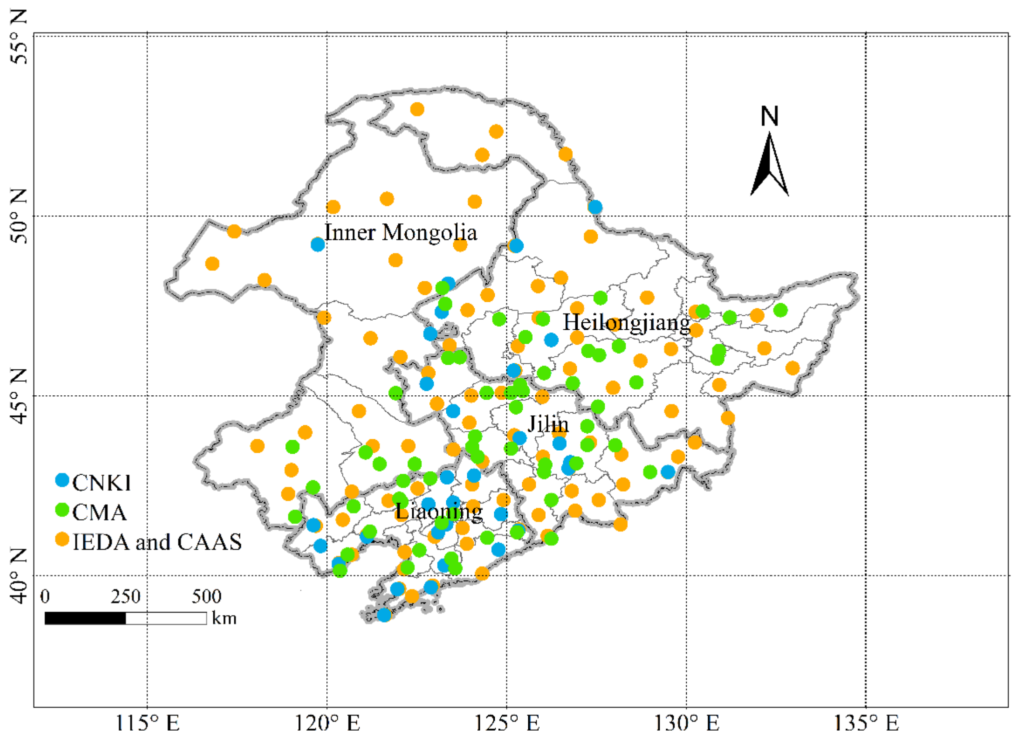

Figure 1. Spatial locations of the original maize phenological records obtained from three base data sets: CNKI, CMA, IEDA, and CAAS.

2.3. Research Methods

2.3.1. Initial Assumptions

The sowing stage of maize is mainly influenced by a combination of geographic and climatic factors, while each subsequent developmental period is influenced by the date of the previous developmental period and any applied management practices, as well as local geographic and climatic factors [17,18]. Given that the focus of this study is on the multi-year average maize development process, differences in management practices in different regions are assumed here to have a negligible effect on the developmental process.

The development of maize from the tasseling stage into the flowering stage and then the silking stage is a continuous process that takes about 5–7 days. However, in the northeast of China, it takes roughly 3–4 days for maize to enter the flowering stage from the tasseling stage and 2–3 days to enter the silking stage from the flowering stage. Therefore, according to the pattern of maize tasseling, flowering, and silking in this region, it is assumed that the flowering stage of maize occurs 3 days after tasseling and the silking stage occurs 2 days after the flowering stage.

2.3.2. Raster Mapping of Phenological Stages

Stepwise multiple regression analysis methods can effectively select the independent variables that contribute significantly to the change in a dependent variable from the many factors that can potentially affect it. An “optimal” regression model can then be built on the identified key independent variables, using observed data of the dependent variable [19,20]. This paper uses this method to fuse three base data sets, starting from the sowing stage, and considers the relationship between the remaining phenological stages (emergence, three-leaf, seven-leaf, jointing, tasseling, flowering, silking, and harvesting) and the date of the previous adjacent phenological stage, the longitude, the latitude, and the altitude.

There are four steps to the phenological data processing performed in this study:

(1) Sowing stage: The 192 maize phenology records used in this paper are known with acceptable accuracy. Hence, there is no need to reconstruct these dates.
(2) Emergence stage: The missing records of the emergence stage were completed by establishing quantitative relationships between the emergence stage and the sowing stage, longitude, latitude, and altitude. Subsequently, the original records were replaced with the model-derived emergence data.
(3) Three-leaf stage, seven-leaf stage, jointing stage, tasseling stage, and harvesting stage: The same method of integration and construction as that of the emergence stage was applied. Only the relationship between the phenological stage and its previous nearest phenological stage, longitude, latitude, and altitude were considered.
(4) Flowering stage and silking stage: It was assumed that the maize entered the flowering stage 1 day after the tasseling stage and the maize entered the silking stage 2 days after the flowering stage.

Based on the processing steps described above, we used the raster calculator and inverse distance weighting method embedded in ArcGIS to spatialize the fused data and the original data and then compared these two data sets to investigate the temporal and spatial distribution patterns of each phenological stage.

2.3.3. Spatial Interpolation Accuracy

After spatial interpolation of the maize phenological data, a validation method was used to assess the accuracy of the interpolations. Validation data were obtained from the 2013 maize phenological data recorded in the CMA base data set, covering seven phenological stages: SW, VE, V3, V7, JT, VT, and R6 (Note: The most recent year recorded in this data set for the tasseling stage was 2002, so data from this year were used for validation purposes for this stage). Mean Absolute Error (MAE) and Root Mean Square Error (RMSE) were used as accuracy evaluation indices, as follows:

$$MAE = \frac{1}{n}\sum_{i=1}^{n}|O_i - P_i| \tag{1}$$

$$RMSE = \sqrt{\frac{1}{n}\sum_{i=1}^{n}(O_i - P_i)^2} \tag{2}$$

where n is the number of data sites, O_i is the actual measured value, and P_i is the predicted value.

3. Results

3.1. Phenological Model

The sowing stage data were considered to be the most accurate and were not required to be reconstructed; hence, a total of eight phenological stage models were derived (Table 2) in order to reconstruct the missing data. Among these, the confidence levels of the VE and R6 models as reflected in the *p*-values were lower than those of the other phenological stages because in the spring the maize sowing stage in Northeast China is influenced by soil moisture deficiencies. These strongly influence the maize germination and maize emergence times, especially in dry years. On the other hand, maize harvesting is largely dependent on machinery, so harvesting times are highly influenced by the degree of agricultural mechanization [21]. In the base data sets, there were cases of early or delayed harvesting by one or two days, resulting in a slightly lower correlation between harvesting and the date of the previous developmental period.

Table 2. Interpolation and reconstruction models for each phenological stage of maize, except for the sowing stage.

	SW	**VE**	**V3**	**V7**	**JT**	**VT**	**FR**	**R1**	**Long (°N)**	**Lat (°E)**	**Alt (m)**	p	R^2
VE	0.51								0.41	0.44	0.01	0.02	0.75
V3		1.24										0.00	0.70
V7			0.96									0.00	0.58
JT				0.88					0.39			0.00	0.62
VT					0.46					0.96		0.00	0.78
FR						+3							
R1							+2						
R6								0.76			0.01	0.02	0.49

Note: SW: sowing stage; VE: emergence stage; V3: three-leaf stage; V7: seven-leaf stage; JT: jointing stage; VT: tasseling stage; FR: flowering stage; R1: silking stage; R6: harvesting stage; Long: longitude; Lat: latitude; Alt: altitude; Phenological stages in DOY.

3.2. Model Accuracy Analysis

Based on the raster map of each phenological stage of maize in Northeast China obtained in Section 2.3.2, and using the extraction analysis function in ArcGIS, the predicted phenological stage data for each inspection site were extracted. Table 3 compares these predicted values with measured values. From the comparison, it can be concluded that the interpolation accuracy of each phenological stage of maize in the northeastern region is in the order: emergence stage > seven-leaf stage > three-leaf stage > jointing stage > harvesting stage > sowing stage > tasseling stage. The interpolation error of the emergence stage is the smallest at 2.81 d, and the interpolation errors of the sowing stage and tasseling stage are the largest at 3.90 d and 4.90 d, respectively. The larger error in the sowing stage validation data is due to the fact that Northeast China is a rain-fed agricultural area. Hence, in drought years, there are cases of early or late sowing due to the influence of soil moisture leading to poor accuracy. The error in the validation of the tasseling stage was because the data were selected from the period 2002 in the CMA data set, which resulted in a large error due to the age of the data, the continuous optimization of maize varieties, and the further improvement of management techniques. Overall, the average interpolation error for all phenological stages was 3.47 d. As a result, the interpolation was good and accurately reflected the process of maize phenology, and the obtained data set of 192 locations containing nine maize phenological stages (Supplementary Materials) can meet the needs of a basic data set for maize meteorological hazard monitoring and early warning.

Table 3. Comparison of measured values and interpolated values at validation sites.

Growth Period	Number of Validation Sites	MAE	RMSE (Days)
SW	61	3.23	3.90
VE	55	2.08	2.81
V3	60	2.40	3.05
V7	59	2.38	2.98
JT	50	2.71	3.28
VT	43	3.91	4.90
R6	34	2.34	3.34

3.3. Raw and Fused Data Correlation Analysis

From Figure 2, it shows that the average values of the raw and fusion data for each phenological stage of maize differed by 0 d, −0.97 d, −0.79 d, −1.17 d, −0.07 d, 0.07 d, −3.01 d, −0.91 d, and −0.11 d, respectively; the degree of dispersion between the raw and fusion data for each phenological stage was generally consistent. A correlation analysis of the raw and fusion data for each phenological stage using SPSS 19.0 showed that the data for the flowering and silking stages constructed by combining experience and regularity had a significant level of correlation with the raw data ($p < 0.05$), indicating that it is reasonable and feasible to construct data for these two stages using experience and regularity. Correlations between raw and fused data reached highly significant levels ($p < 0.01$) for the other phenological stages, except for the sowing stage, so it can be concluded that the data set obtained in this paper achieves the aim of enriching maize phenological data while maintaining the scientific validity of the raw data.

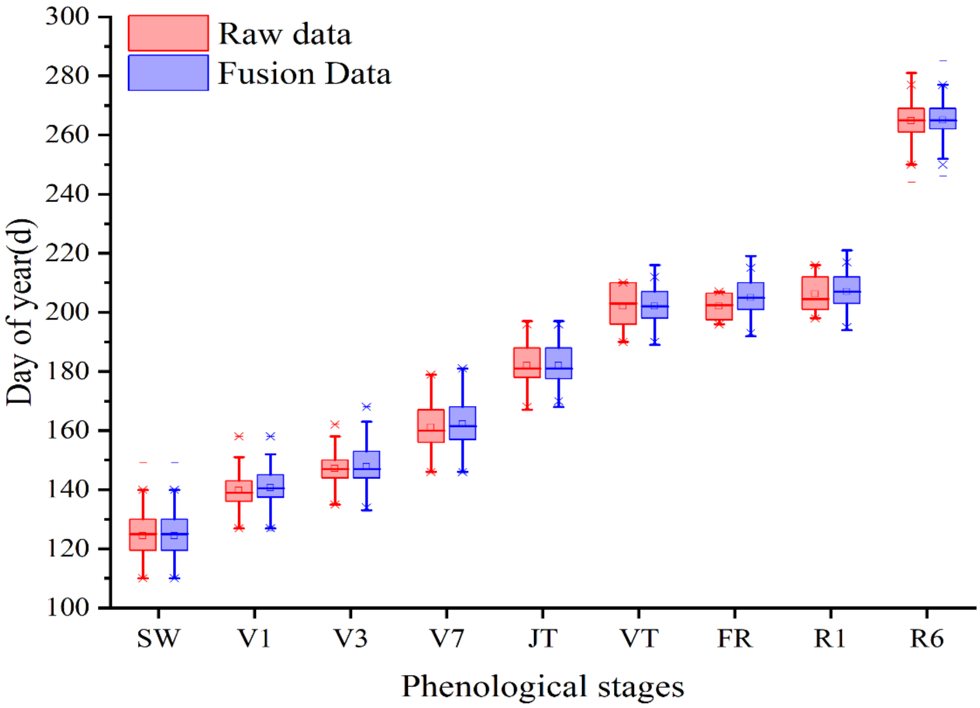

Figure 2. Comparison of raw and fused data for each phenological stage.

3.4. Phenological Maps

3.4.1. Sowing Stage (SW)

Soil temperature and soil moisture are the main factors affecting the sowing of maize [22,23]. However, there is a widespread low temperature and lack of water resources in Northeast China, especially in Heilongjiang Province in the northern part of the region [24,25]. Therefore, the primary consideration when sowing maize in most areas is the ambient temperature conditions [26]. Maize sowing demands ambient temperatures higher than 10 °C [27], and even if the soil moisture is insufficient, it can be sown in time to wait for rainfall to replenish the soil moisture.

The spatial distribution of the sowing period (Figure 3) is well aligned with the climatic conditions of the spring (higher temperatures at lower latitudes compared to higher latitudes), with a maximum difference of 39 days from southern Liaoning to northern Heilongjiang. Sowing starts in mid-April in southwestern Liaoning; the rest of Liaoning, most of Jilin, and eastern Inner Mongolia in late April; and in early May in most of Heilongjiang and Inner Mongolia.

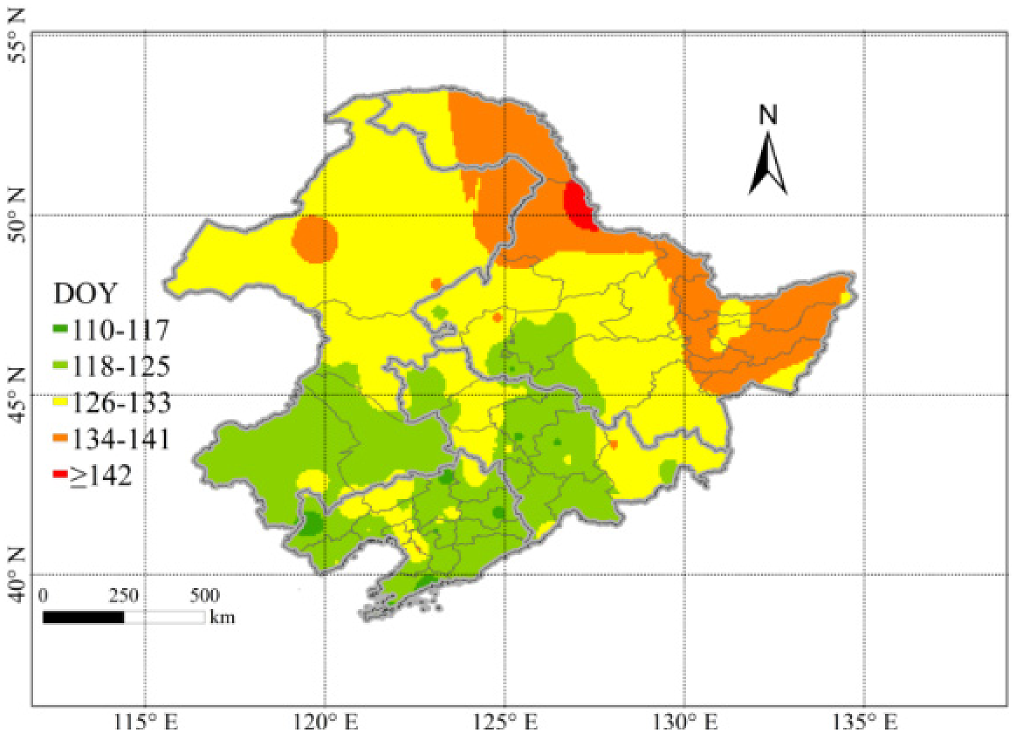

Figure 3. Maize sowing stage (SW) in Northeast China. Note: as all sowing dates were known there was no requirement for a reconstructed data set.

3.4.2. Emergence Stage (VE)

Soil moisture is the most crucial factor affecting the emergence of maize. Before moisture conditions are met, drought can cause maize to fail to germinate. Therefore, the maize emergence period varies significantly from year to year [28].

The spatial interpolation of the emergence stage (Figure 4) reveals large differences in seedling emergence due to different soil moisture conditions in the different regions. The maximum interval between seedling emergence between regions is 33 days. In southwestern Liaoning, the seedling emergence occurs in early May; in the rest of Liaoning, eastern Inner Mongolia, most of Jilin, and western Heilongjiang in mid-May; and in the rest of the regions in late May. The remaining regions enter the seedling stage in late May.

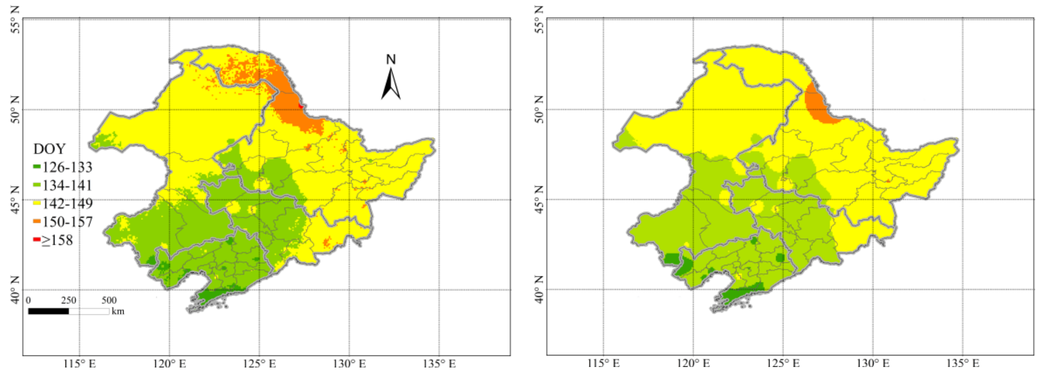

(**a**) (**b**)

Figure 4. Maize emergence stage (VE) in Northeast China ((**a**) fusion data; (**b**) original data).

3.4.3. Three-Leaf Stage (V3)

When seeds are depleted of nutrients, the maize will switch from autotrophic to heterotrophic, representing the entry into the three-leaf stage. The maximum difference in the time interval for entering the trifoliate stage is 27 days in different regions (Figure 5). The spatial distribution characteristics of entry into the three-leaf stage in each geographical region are similar to those of the emergence stage: mid-May in southwestern Liaoning; late May in the rest of Liaoning, eastern Inner Mongolia, most of Jilin, and western Heilongjiang; and late May in northeastern Inner Mongolia and northern Heilongjiang.

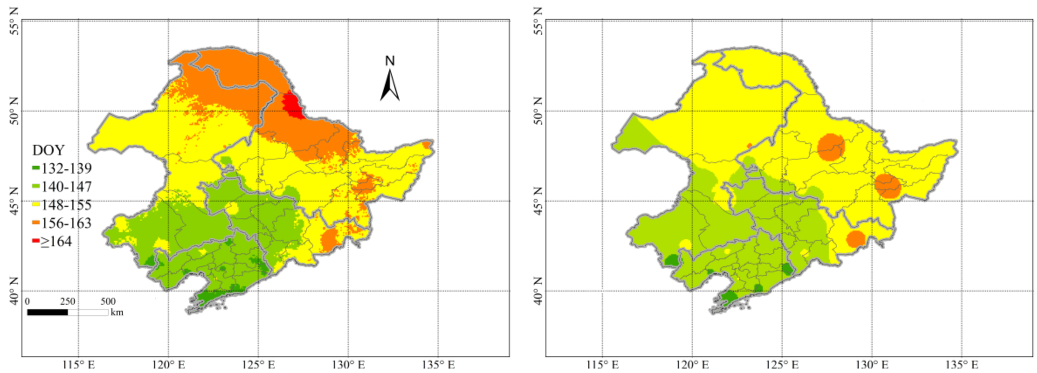

(**a**) (**b**)

Figure 5. Three-leaf stage (V3) of maize in Northeast China ((**a**) fusion data; (**b**) original data).

3.4.4. Seven-Leaf Stage (V7)

The seven-leaf stage is a sign that maize has entered the vigorous nutritional growth stage. Maize growth in southwestern Liaoning occurs the seven-leaf stage in late May (Figure 6); followed by other parts of Liaoning, eastern Inner Mongolia, most of Jilin, and western Heilongjiang in mid-to early June; and parts of northeastern Inner Mongolia and northern Heilongjiang in late June.

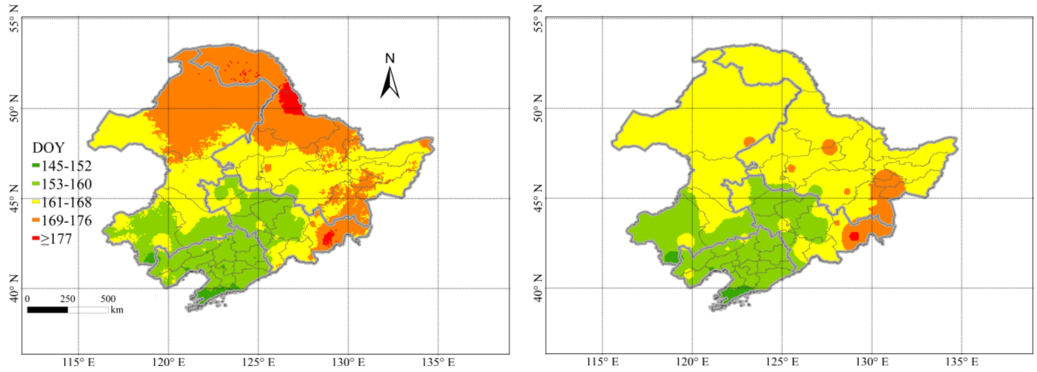

(**a**) (**b**)

Figure 6. Seven-leaf stage (V7) of maize in Northeast China ((**a**) fusion data; (**b**) original data).

3.4.5. Jointing Stage (JT)

The jointing stage transforms nutritional growth into reproductive growth [29]. With the acceleration of maize growth and the development process, the difference of developmental time between different regions is further reduced. The distribution is characterized as follows (Figure 7): growth and development of maize in Liaoning, western Jilin, and eastern Inner Mongolia enter the jointing stage in late June; the northeastern Inner Mongolia and northern Heilongjiang enter the jointing stage in mid-July; and most of the rest of the regions enter the jointing stage in July.

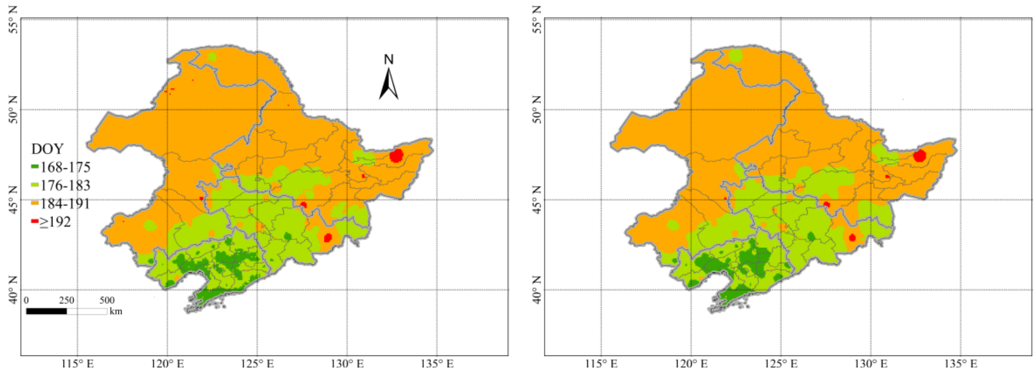

(**a**) (**b**)

Figure 7. Maize jointing stage (JT) in Northeast China ((**a**) fusion data; (**b**) original data).

3.4.6. Tasseling Stage (VT)

The tasseling stage marks the beginning of the reproductive growth phase, where maize water demand reaches its maximum. If maize suffers from drought at this stage, it will lead to a certain degree of yield reduction. Most of Liaoning, central Jilin, and eastern Inner Mongolia enter the tasseling stage in mid-July (Figure 8); it is early August for Inner Mongolia and northern Heilongjiang; and late July for most of the rest of the areas.

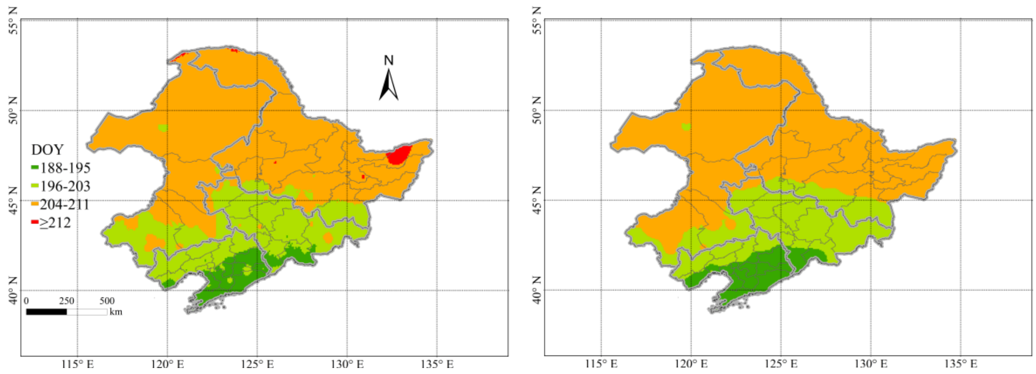

(**a**) (**b**)

Figure 8. Maize tasseling stage (VT) in Northeast China ((**a**) fusion data; (**b**) original data).

3.4.7. Flowering Stage (FR)

The small amount of flowering data in the original data resulted in poor spatial interpolation and no reference values for validation. However, establishing the flowering data set was necessary because flooding disasters are prone to occur during the flowering stage of maize, which causes irreparable effects on maize yield. Therefore, the flowering stage data set was established.

The spatial distribution of the flowering stage and tasseling stage are similar (Figure 9): most of Liaoning and central Jilin, as well as eastern Inner Mongolia, enter the flowering stage in mid-July, while Inner Mongolia and northern Heilongjiang enter the flowering stage in early August. Most of the remaining areas enter the flowering stage in late July.

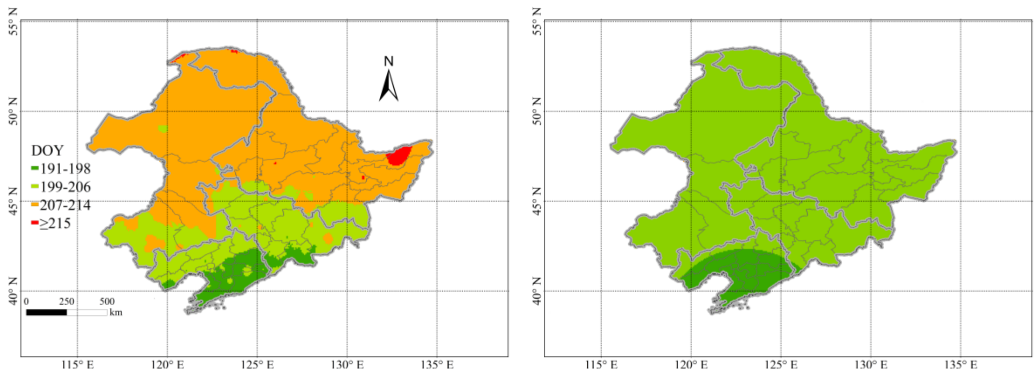

(**a**) (**b**)

Figure 9. Maize flowering stage (FR) in Northeast China ((**a**) fusion data; (**b**) original data).

3.4.8. Silking Stage (R1)

There are less available raw data for the silking stage than for other stages, but the construction of the silking stage data set is necessary, as this stage is one of the key phenological stages that determine the final yield of maize. The silking stage data set was obtained by combining the growth and development pattern of maize based on the flowering stage data.

The spatial distribution of the silking stage (Figure 10) is similar to the distribution characteristics of the flowering stage. Most of Liaoning, central Jilin, and eastern Inner Mongolia enter the silking stage in mid-July; Inner Mongolia and northern Heilongjiang enter in early August; and most remaining areas in late July.

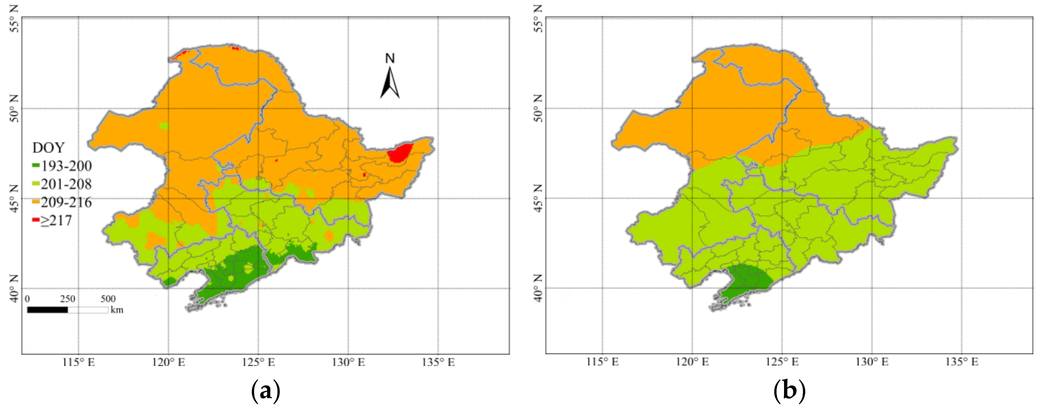

Figure 10. Maize silking stage (R1) in Northeast China ((**a**) fusion data; (**b**) original data).

3.4.9. Harvesting Stage (R6)

When the bract color of maize turns white and faded, it marks the arrival of the harvesting stage. Since harvesting is subject to human influence and there are early or late harvesting cases, the fused data more accurately reflect the harvesting stage of maize.

The spatial distribution of the harvesting process (Figure 11) is characterized by the majority of Liaoning Province, the southern part of Jilin Province, and some areas in the eastern part of Inner Mongolia entering harvesting in mid-September; most of the remaining areas maturing in late September; and some areas in northern Heilongjiang and northeastern Inner Mongolia enter harvesting in early October.

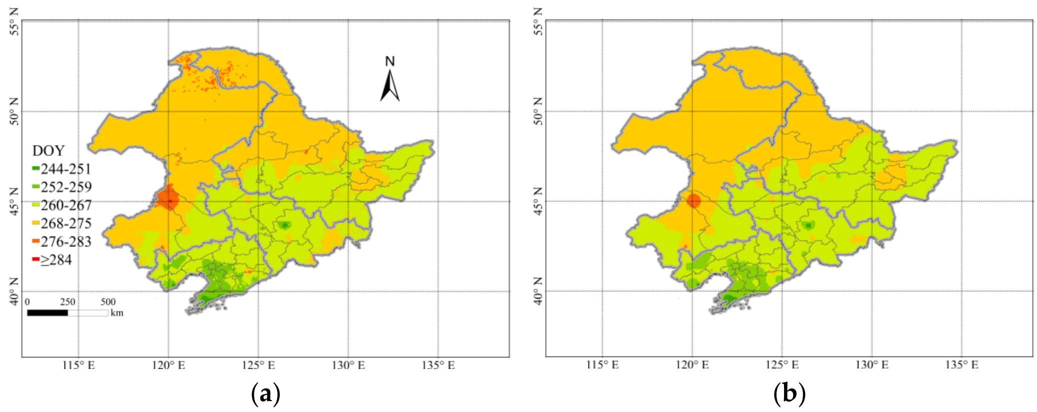

Figure 11. Maize harvesting stage (R6) in Northeast China ((**a**) fusion data; (**b**) original data).

4. Discussion

With the development of remote sensing technology, it has become a trend to use satellite remote sensing technology to monitor crop growth. Depending on the cropping system and planting time of various crops in China, several maize phenological stages (V3, heading, and maturity stage) can be obtained in a targeted manner with remote sensing monitoring [30]. The phenological data obtained through remote sensing monitoring can be combined with the phenological models gained by the authors for further extrapolation to obtain additional phenological data. Compared to observing the spatial distribution of maize phenological stages through remote sensing, the use of in situ phenological stage records combined with GIS to obtain the spatial distribution of maize phenological stages has the advantage of higher accuracy and inclusion of many phenological stages. Regression analysis can solve problems associated with incomplete records and few recording sites in original data sets. By comparing the spatial distributions of the fusion data set (Figure 4a, Figure 5a, Figure 6a, Figure 7a, Figure 8a, Figure 9a, Figure 10a, Figure 11a) and the original data set (Figure 4b, Figure 5b, Figure 6b, Figure 7b, Figure 8b, Figure 9b, Figure 10b,

Figure 11b) for each phenological period, it is concluded that the zonal patterns and spatial detail derived from the fused data set for each phenological period are better than those derived from the original base data.

The phenological process of maize in each region results from a combination of the physiological process of the maize germplasm itself and external environmental conditions. This study shows that maize in the northeast of China generally starts to be sown in mid to late April and matures in mid to late September, and in some areas in early October. The phenological stages progress gradually from southwest to northeast, but the time intervals between each phenological stage vary: sowing stage of 110–149 d, emergence stage of 126–159 d, three-leaf stage of 133–169 d, seven-leaf stage of 146–182 d, jointing stage of 168–197 d, tasseling stage of 189–216 d, flowering stage of 192–219 d, silking stage of 194–221 d, and harvesting stage of 245–285 d. Additionally, there is a clear trend of later phenology at higher latitudes in the spatial distributions. Liu, Y. et al. [21] concluded in the process of their study that the northeast corn of each phenophase time range is stated as follows: sowing stage of 110–124 d, emergence stage of 127–141 d, three-leaf stage of 133–148 d, seven-leaf stage of 152–165 d, jointing stage of 174–185 d, tasseling stage of 198–205 d, and harvesting stage of 254–264 d. Compared with the data range we collected, our collected data range is more extensive, mainly because the author studied a wider area. Luo, Y. et al. [30]. found by using remote sensing observations that the average three-leaf, tasseling, and maturity stage development times of maize in Northern China were 142.4 d, 214.3 d, and 254.9 d, respectively, which is consistent with some of the results outlined in this paper. Zhang, J. et al. [31]. elucidated that the growth process of maize in high latitudes was lagging behind in low latitudes, which resonated with our findings that the development process of maize tended to have a later growth period with higher latitudes.

By fusing different maize phenological data sets and spatially mapping each phenological period in Northeast China, it is possible to better guide the planting and production of maize in the region and provide a basis for decision making in mitigating agrometeorological disasters as well as aiding the selection and breeding of suitable maize varieties for planting. Climatic conditions, such as temperature, sunshine hours, and rainfall, are the main factors affecting maize's growth and phenological processes [32–34], Wheat phenology has changed in response to changes in climatic resources, and according to research, future warming will lead to earlier phenology for maize [35,36]. The main factors influencing climate are the latitudinal position, atmospheric circulation, land and sea distribution, ocean currents, and topography. Different geographical locations have different climates. The higher the altitude, the lower the temperature. The higher the latitude, the lower the angle of sunlight, and the less heat it receives, the colder the climate. The distribution of land and sea and the contrast between land and sea bring about differences in dryness and humidity, creating zones of dryness and humidity (longitude zones), and the climate changes regularly with changes in dryness and humidity [37,38]. Geographical factors can reflect the climatic characteristics of different regions. In this paper, only geographical factors (latitude, longitude, and altitude), along with the date of the previous phenological period, were considered as factors affecting the phenological process. The effects of precipitation, temperature, and soil texture were not taken into account. Owing to the development of maize seed production technology, the range of heat and moisture toleration of this crop is increasing. The fusion of maize developmental data sets as demonstrated here, combined with an increase in available in situ recorded data, will allow planners to fully consider the influence of varietal differences and other meteorological factors (humidity, etc.) on maize growth and development in the future [39]. Detailed multi-site maize phenology data meet the demands for data on maize cultivation and breeding in the context of global warming and for early warning and prediction of regional meteorological hazards. For example, most studies on the climatic suitability of maize were limited to a few growths and developmental stages (e.g., germination to emergence, emergence to jointing, jointing to tasseling, and tasseling to maturity) [3]. However, with the data set obtained by the authors, this research can be conducted at a finer scale and extended to the phenological scale. The number of points used in spatial interpolation determines the accuracy of the interpolation results. Obviously, the more the number of points, the higher the accuracy of the interpolation results [40]. In this paper, the authors collected three sources of data on the phenological stages, and the accuracy of the final results can meet the basic data requirements. In future studies, the authors will take measures, such as field investigation, to further increase the number of raw data and more abundant data source locations.

5. Conclusions

In this study, the data from different sources of phenological stages were adopted in a mathematical and statistical analysis to finally obtain a completely new data set with 192 locations and nine maize phenological stages. The correlation among the newly constructed flowering and silking stage data and the original data was significant ($p < 0.05$), while the correlation among the other phenological stages and the original data was highly significant ($p < 0.01$). The errors of the emergence stage, three-leaf stage, seven-leaf stage, jointing stage, tasseling stage, and harvesting stage data were 3.90 d, 2.81 d, 3.05 d, 2.98 d, 3.28 d, 4.90 d, and 3.34 d, respectively, with an average error of 3.47 d. The accuracy is up to standard of agricultural disaster prevention and mitigation. The time range of each phenological stage of maize in Northeast China was sowing stage of 110–149 d, emergence stage of 126–159 d, three-leaf stage of 133–169 d, seven-leaf stage of 146–182 d, jointing stage of 168–197 d, tasseling stage of 189–216 d, flowering stage of 192–219 d, silking stage of 194–221 d, and harvesting stage of 245–285 d. In addition, the spatial distributions show a clear trend of later phenology at higher latitudes.

In future studies, it will be envisaged to introduce climatic variables in the phenological period models, which will assist in improving the accuracy of the models. In addition, remote sensing technology is becoming more accurate in monitoring crop growth, and combining remote sensing monitoring results with the phenology model may lead to more locations with phenology data, which will help planners to make reasonable adjustments to maize varieties and cropping patterns.

Supplementary Materials: The following supporting information can be downloaded at: https://www.mdpi.com/article/10.3390/agronomy12102585/s1.

Author Contributions: X.W. analyzed the data and prepared the draft manuscript. H.Z. and C.S. provided comments and substantially revised the manuscript. S.Y. conceived the study, provided comments, and revised the manuscript. X.L., J.G. and W.S. prepared the maize phenological data and revised the manuscript. All authors have read and agreed to the published version of the manuscript.

Funding: The Ministry of Science and Technology (MOST) of China supported this work (grant number: 2017YFD0300400).

Data Availability Statement: The maize phenology data obtained for the Northeast China study were uploaded as Supplementary Materials. Results related to maize phenology data from the Huang Huaihai region of China have also been published [41].

Conflicts of Interest: The authors declare no conflict of interest.

References

1. Akram, M.A.; Wahid, A.; Abrar, M.; Manan, A.; Naeem, S.; Zahid, M.A.; Gilani, M.M.; Paudyal, R.; Gong, H.Y.; Ran, J.Z.; et al. Comparative study of six maize (*Zea mays* L.) Cultivars concerning cadmium uptake, partitioning and tolerance. *Appl. Ecol. Environ. Res.* **2021**, *19*, 2305–2331. [CrossRef]
2. Shah, T.R.; Prasad, K.; Kumar, P. Maize—A potential source of human nutrition and health: A review. *Cogent Food Agric.* **2016**, *2*, 1166995. [CrossRef]
3. Zhao, J.; Guo, J.; Xu, Y.; Mu, J. Effects of climate change on cultivation patterns of spring maize and its climatic suitability in Northeast China. *Agric. Ecosyst. Environ.* **2015**, *202*, 178–187. [CrossRef]
4. Anjum, S.A.; Ehsanullah; Ashraf, U.; Tanveer, M.; Qamar, R.; Khan, I. Morphological and phenological attributes of maize affected by different tillage practices and varied sowing methods. *Am. J. Plant Sci.* **2014**, *5*, 1657–1664. [CrossRef]

5. Cai, Q.; Zhang, Y.; Sun, Z.; Zheng, J.; Bai, W.; Zhang, Y.; Liu, Y.; Feng, L.; Feng, C.; Zhang, Z.; et al. Morphological Plasticity of Root Growth under Mild Water Stress Increases Water Use Efficiency without Reducing Yield in Maize. *Biogeosciences* **2017**, *14*, 3851–3858. [CrossRef]
6. Dabrowska-Zielinska, K.; Malinska, A.; Bochenek, Z.; Bartold, M.; Gurdak, R.; Paradowski, K.; Lagiewska, M. Drought model diss based on the fusion of satellite and meteorological data under variable climatic conditions. *Remote Sens.* **2020**, *12*, 2944. [CrossRef]
7. Zhang, A.; Jia, G. Monitoring meteorological drought in semiarid regions using multi-sensor microwave remote sensing data. *Remote Sens. Environ.* **2013**, *134*, 12–23. [CrossRef]
8. Gong, Y.; Huang, W.; Wang, J.; Xu, X.; Yan, G. Progress and application of integrating GIS and RS technology to monitor and forecast crop diseases and pests. *Trans. Chin. Soc. Agric. Eng.* **2008**, *24*, 331–336.
9. Xue-Jun, C.; Guang-Cai, C.; Qun, S.; Dong-Bin, W.; Jing, C.; Ya-Xiong, Y.; Jie, L.; Wei, L. Altitude effects on maize growth period and quality traits. *Acta Ecol. Sin.* **2013**, *33*, 233–236. [CrossRef]
10. Liu, Y.; Zhang, L.; Yin, X.; Zou, X.; Chen, F. Influence of climate change and mechanized harvest- 394 ing on the maize (*Zea mays* L.) Planting and northern limits in northeast China. *J. Sci. Food* **2020**, *101*, 3889–3897. [CrossRef]
11. Mo, F.; Sun, M.; Liu, X.Y.; Wang, J.Y.; Zhang, X.C.; Ma, B.L.; Xiong, Y.C. Phenological responses of spring wheat and maize to changes in crop management and rising temperatures from 1992 to 2013 across the Loess Plateau. *Field Crops Res.* **2016**, *196*, 337–347. [CrossRef]
12. Xiao, D.; Zhang, Y.; Bai, H.; Tang, J. Trends and climate response in the phenology of crops in northeast China. *Front. Earth Sci.* **2021**, *9*, 811621. [CrossRef]
13. Tao, F.; Yokozawa, M.; Xu, Y.; Hayashi, Y.; Zhang, Z.J.A. Climate changes and trends in phenology and yields of field crops in China, 1981–2000. *Agric. For. Meteorol.* **2006**, *138*, 82–92. [CrossRef]
14. Jiang, L.Y.; Yang, H.Z.; Qiao, G.X.; Zhang, G.X.; Zhong, T.S.; Li, X.T. Species diversity, fauna and distribution of aphids in Northeast China. In Proceedings of the 8th International Symposium on Aphids, Catania, Italy, 8–12 June 2009; pp. 199–204.
15. Zhao, J.; Yang, X.; Liu, Z.; Lv, S.; Wang, J.; Dai, S. Variations in the potential climatic suitability distribution patterns and grain yields for spring maize in Northeast China under climate change. *Clim. Chang.* **2016**, *137*, 29–42. [CrossRef]
16. Yang, X.; Ming, B.; Tao, H.; Wang, P. Spatial distribution characteristics and impact on spring maize yield of drought in Northeast China. *Chin. J. Eco-Agric.* **2015**, *23*, 758–767.
17. Tian, B.; Zhu, J.; Nie, Y.; Xu, C.; Meng, Q.; Wang, P. Mitigating heat and chilling stress by adjusting the sowing date of maize in the North China Plain. *J. Agron. Crops Sci.* **2019**, *205*, 77–87. [CrossRef]
18. Fang, Q.; Wang, Y.; Uwimpaye, F.; Yan, Z.; Li, L.; Liu, X.; Shao, L. Pre-sowing soil water conditions and water conservation measures affecting the yield and water productivity of summer maize. *Agric. Water Manag.* **2021**, *245*, 106628. [CrossRef]
19. González-Longatt, F.; Medina, H.; González, J.S. Spatial interpolation and orographic correction to estimate wind energy resource in Venezuela. *Renew. Sustain. Energy* **2015**, *48*, 1–16. [CrossRef]
20. Kim, E.Y.; Koh, D.C.; Ko, K.S.; Yeo, I.W. Prediction of nitrate contamination of groundwater in the northern nonsan area using multiple regression analysis. *J. Soil Groundw. Environ.* **2008**, *13*, 57–73.
21. Liu, Y.; Zhang, J.; Pan, T.; Ge, Q. Assessing the adaptability of maize phenology to climate change: The role of anthropogenic-management practices. *J. Environ. Manag.* **2021**, *293*, 112874. [CrossRef]
22. Yin, W.; Feng, F.; Zhao, C.; Yu, A.; Hu, F.; Chai, Q.; Gan, Y. Integrated double mulching practices optimizes soil temperature and improves soil water utilization in arid environments. *Int. J. Biometeorol.* **2016**, *60*, 1423–1437. [CrossRef] [PubMed]
23. Dai, Z.; Hu, J.; Fan, J.; Fu, W.; Hao, M. No-tillage with mulching improves maize yield in dryland farming through regulating soil temperature, water and nitrate-N. *Agric. Ecosyst. Environ.* **2021**, *309*, 107288. [CrossRef]
24. Chu, Z.; Guo, J.P.; Zhao, J.F. Impacts of future climate change on agroclimatic resources in Northeast China. *J. Geogr. Sci.* **2017**, *27*, 1044–1058. [CrossRef]
25. Zhao, J.; Zhang, J.Q.; Liu, X.P.; Li, Y.; Wang, R. Impacts of northern expansion of typical corn planting regions in china under the background of climate warming and spatial evolution of cold damage. *Aebmr Adv. Econ.* **2018**, *66*, 205–210. [CrossRef]
26. Finch-Savage, W.E.; Dent, K.C.; Clark, L.J. Soak conditions and temperature following sowing influence the response of maize (*Zea mays* L.) seeds to on-farm priming (pre-sowing seed soak). *Field Crops Res.* **2004**, *90*, 361–374. [CrossRef]
27. Chen, C.; Qian, C.; Deng, A.; Zhang, W. Progressive and Active Adaptations of Cropping System to Climate Change in Northeast China. *Eur. J. Agron.* **2012**, *38*, 94–103. [CrossRef]
28. Kumar, R.; Farooq, Z.; Nabi, S.; Jhajharia, D. Ecohydrological modeling of irrigation scheduling of maize using time series analysis in the temperate region of Kashmir valley, India. *Water Supply* **2015**, *15*, 727–735. [CrossRef]
29. Cai, Y.; Zhang, S.; Cai, K.; Huang, F.; Pan, B.; Wang, W. Cd accumulation, biomass and yield of rice are varied with silicon application at different growth phases under high concentration cadmium-contaminated soil. *Chemosphere* **2020**, *242*, 125128. [CrossRef]
30. Luo, Y.; Zhang, Z.; Chen, Y.; Li, Z.; Tao, F. ChinaCropPhen1km: A high-resolution crop phenological dataset for three staple crops in China during 2000–2015 based on leaf area index (LAI) products. *Earth Syst. Sci. Data.* **2020**, *12*, 197–214. [CrossRef]
31. Zhang, J.; Feng, L.; Yao, F. Improved maize cultivated area estimation over a large scale combining MODIS–EVI time series data and crop phenological information. *ISPRS J. Photogramm. Remote Sens.* **2014**, *94*, 102–113. [CrossRef]
32. Ding, Y.; He, X.; Zhou, Z.; Hu, J.; Cai, H.; Wang, X.; Li, L.; Xu, J.; Shi, H. Response of vegetation to drought and yield monitoring based on NDVI and SIF. *CATENA* **2022**, *219*, 106328. [CrossRef]

33. Safian, N.; Naderi, M.R.; Torabi, M.; Soleymani, A.; Salemi, H.R. Corn (*Zea mays* L.) And sorghum (*Sorghum bicolor* (L.) Moench) yield and nutritional quality affected by drought stress. *Biocatal. Agric. Biotechnol.* **2022**, 102486. [CrossRef]
34. Yang, C.; Lei, H. Climate and management impacts on crop growth and evapotranspiration in the north china plain based on long-term eddy covariance observation. *Agric. For. Meteorol.* **2022**, *325*, 109147. [CrossRef]
35. Tao, F.; Xiao, D.; Zhang, S.; Zhang, Z.; Roetter, R.P. Wheat Yield Benefited from Increases in Minimum Temperature in the Huang-Huai-Hai Plain of China in the Past Three Decades. *Agric. For. Meteorol.* **2017**, *239*, 1–14. [CrossRef]
36. Xiao, D.; Liu, D.L.; Wang, B.; Feng, P.; Bai, H.; Tang, J. Climate change impact on yields and water use of wheat and maize in the north china plain under future climate change scenarios. *Agric. Water Manag.* **2020**, *238*, 106238. [CrossRef]
37. Jing, Y.; Liu, J.; Wan, L. Comparison of climate responses to orbital forcing at different latitudes during the holocene. *Quat. Int.* **2022**, *622*, 65–76. [CrossRef]
38. Guo, M.; Wu, C.; Peng, J.; Lu, L.; Li, S. Identifying contributions of climatic and atmospheric changes to autumn phenology over mid-high latitudes of north-ern hemisphere. *Glob. Planet. Chang.* **2021**, *197*, 103396. [CrossRef]
39. Wang, T.; Li, N.; Li, Y.; Lin, H.; Yao, N.; Chen, X.; Li Liu, D.; Yu, Q.; Feng, H. Impact of climate variability on grain yields of spring and summer maize. *Comput. Electron. Agric.* **2022**, *199*, 107101. [CrossRef]
40. Radočaj, D.; Jug, I.; Vukadinović, V.; Jurišić, M.; Gašparović, M. The effect of soil sampling density and spatial autocorrelation on interpolation accuracy of chemical soil properties in arable cropland. *Agronomy* **2021**, *11*, 2430. [CrossRef]
41. Wang, X.; Li, X.; Shi, W.; Zhao, H.; Sun, C.; You, S. Study of mapping of maize growth period in Huang-Huai-Hai region. *JiangSu Agric. Sci.* **2022**, accepted.